CALIFORNIA INSTITUTE OF TECHNOLOGY
PASADENA, CALIFORNIA 91125
March 24, 2008

To: MWA-LFD Collaboration
From: Judd D. Bowman
Subject: Analysis of Drift Scans from 32T-X2.5 and Characterization of Revised Dipole Designs

The X2.5 expedition to the 32T sub-array was conducted March 5 through 9, 2008, by Merv Lynch, David Herne, and Jamie Stevens. Originally intended as a brief infrastructure "housekeeping" expedition, the scope of X2.5 was increased after schedule revisions delayed subsequent expeditions until April. As a result, the primary goal of X2.5 became to test new hardware solutions for the spike in system temperature at ~200 MHz that was discovered from analysis of the drift scan measurements of X1 in December, 2007.

Detailed numerical electromagnetic simulation of the MWA antenna tiles following X1 identified the source of the problem as a resonance between currents in the vertical elements of neighboring dipole arms (see EDGES Memo #37 and #38). Revised dipole designs were developed using additional modeling to reduce the effects of any such resonances. In early 2008, a candidate design was selected for hardware testing and fabrication of 32 new dipole arms (enough to modify one antenna tile) was completed in February. The candidate dipole design is based on a small modification to the dimensions of the original "bowtie" design so that it is slightly shorter and wider than the original design (see Figure 1).

During X2.5, one tile was modified to test the candidate dipole design by replacing the existing dipole arms with the newly fabricated ones. This version of the tile is shown in Figure 2 and will be labeled as the "ShortWide" test case in this document. A second version of the candidate dipole design was also tested during X2.5. This version is shown in Figure 3 and is the same as the "ShortWide" design, but with the addition of small horizontal arms along the mid-line of each bowtie that extend beyond the vertical elements. According to simulations, the horizontal "stubs" should improve the impedance match of the new dipole design at lower frequencies. This version is labeled "ShortWideStubs". Drift scans were acquired during X2.5 for both versions of the candidate design, along with an unmodified tile (labeled "OldBowtie") for direct comparison. The results of analyzing these drift scans are presented below.

In previous analyses (see MWA-LFD memos on X1 and X2 drift scans), a canonical ideal dipole response was used to simulate the antenna pattern on the sky. Similarly, a simple frequency-scaling of the Haslam et al. 1982 map from 408 MHz to the observed frequency with a power law spectral index of β=-2.6 was used to simulate the sky brightness temperature. For X2.5, I have replaced both of these simple models. To improve the modeled antenna response patterns, Randall Wayth and Chris Williams provided the output of WIPL-D numerical electromagnetic simulations for a full MWA antenna tile for each dipole design tested during X2.5. To improve the modeled sky, I used Angelica de Oliveira-Costa's global sky model (de Oliveira-Costa et al. 2008) derived from interpolating between measured all-sky maps at many frequencies using a principal components analysis. A comparison of the modeled drift scan curves generated with the new and old models is shown in Figures 4-8 at four characteristic frequencies.

The primary results of the drift scan analyses (for both the old and new antenna/sky models) are shown in Figures 9-12, and three appendices present plots summarizing additional aspects of the analyses for the drift scans associated with each dipole design.

So what do we learn from these measurements? First, and most importantly, we can conclude that the new "ShortWide" and "ShortWideStubs" dipole designs do eliminate the 200 MHz resonance-induced spike in the system temperature. Second, by comparing the overall amplitude of the system temperatures in Figure 9 to similar figures from X1, I believe it is possible to conclude that the new (non-ED) beamformer (which was used in X2.5 and in X2, but not in X1) introduces considerably less second-stage noise than the old prototype (ED) beamformer. Unfortunately, the X2 drift scan results were probably corrupted by solar contamination and are not particularly useful for this purpose. From Brian Corey (March 20, 2008):

> *The new (not ED) beamformer used in X2 and X2.5 has all 16 channels on one PCB and with an amplifier at each input to improve its noise performance. It is a prototype in the sense that it was the first with the 16-channel boards and with the new communications protocol over RS485. There have been many subsequent changes made to the layout and BF RX I/O connections for the current [final?] version of the beamformer, which will be used first in X3.*

Finally, given the strong dependence of the overall amplitudes of the derived system temperatures on the specific details of the antenna and sky models (as seen by the differences between Figures 9 and 10), I believe we cannot, with confidence, quote an absolute system temperature or an absolute second-stage noise contribution from these (or earlier X1 or X2) drift scans.

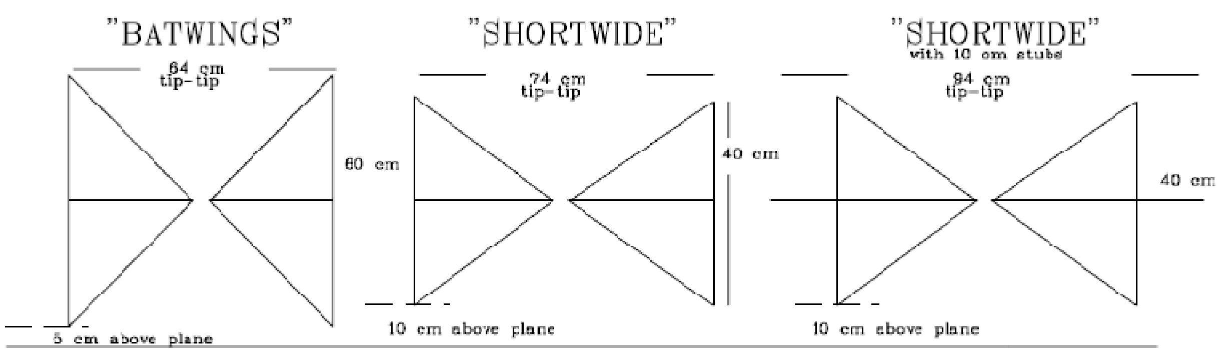

Figure 1. Schematics of the three dipole designs tested during X2.5. From left to right, the drawings correspond to the "OldBowties", "ShortWide", and "ShortWideStubs" labels used in this memo. Reproduced from EDGES Memo #38.

Figure 2. Photograph of the “ShortWide” dipoles. Credit: David Herne

Figure 3. Photograph of the “ShortWideStubs” dipoles. Credit: David Herne

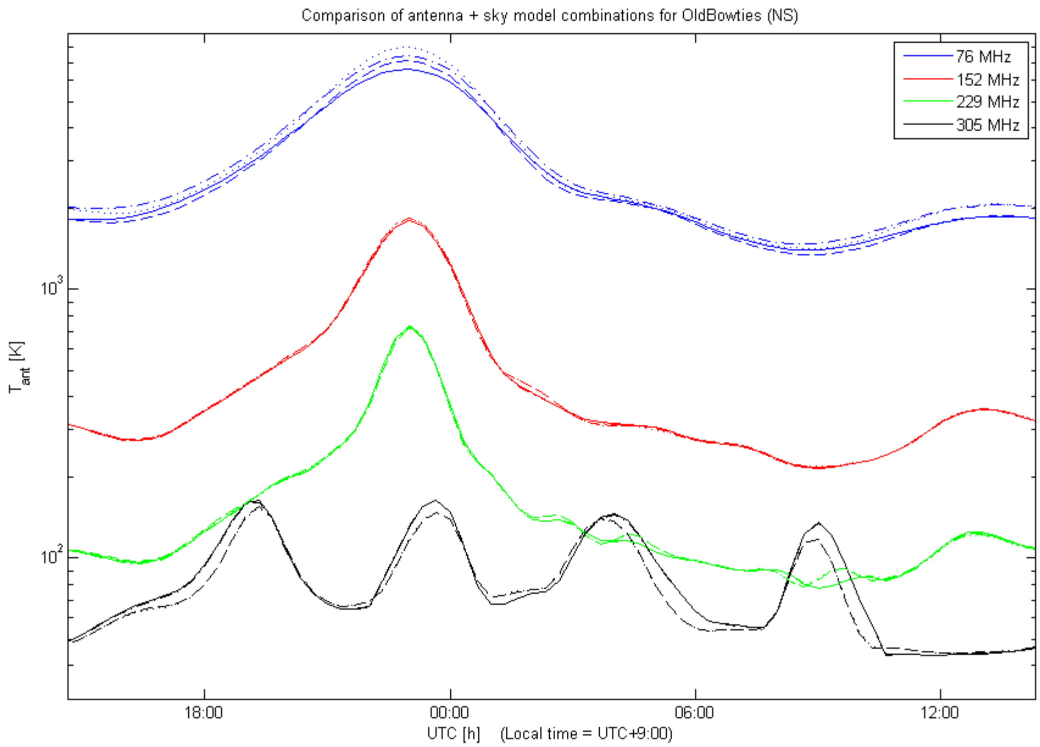

Figure 4. Simulated drift scans at the four frequencies indicated by the color lines. The solid lines are for the original model of ideal dipoles + Haslam map. The dashed lines are for the ideal dipoles + GSM. The dash-dot lines are for the WIPL + Haslam map. And the dotted lines are for the new model of WIPL + GSM. In most cases, the different curves are nearly identical. This indicates that the net effect of using the crude models in X1 and X2 should be minimal. The two most notable differences occur at the low- and high- frequency extremes. At the 76 MHz scan, the amplitude of the peak of the scan (when the Galactic center transits) varies between the models by hundreds of K (see Figure 7 for a plot of the fractional deviations). We will see later that this causes the system temperature estimates to systematically differ between the models at low frequencies. There a couple possible causes to this. I have noticed that Angelica's GSM model is nearly identical to a simple -2.6 scaling of the Haslam map at high Galactic latitudes, but differs substantially at several locations in the Galactic plane. This may be the origin of the large difference at low frequencies. A significant difference in the predicted beam shape (or gain) of the antenna tiles between models could also contribute. The differences in the 305 MHz are the second most noticeable feature. In this case, the four peaks are due to the Galactic center and Sun passing through the sidelobes of the antenna beam, since the response toward zenith is below the sidelobe response at this frequence. The difference between the models is divided along antenna models and is due to a small shift in the position of the beam sidelobes between the ideal dipole model and the WIPL antenna pattern.

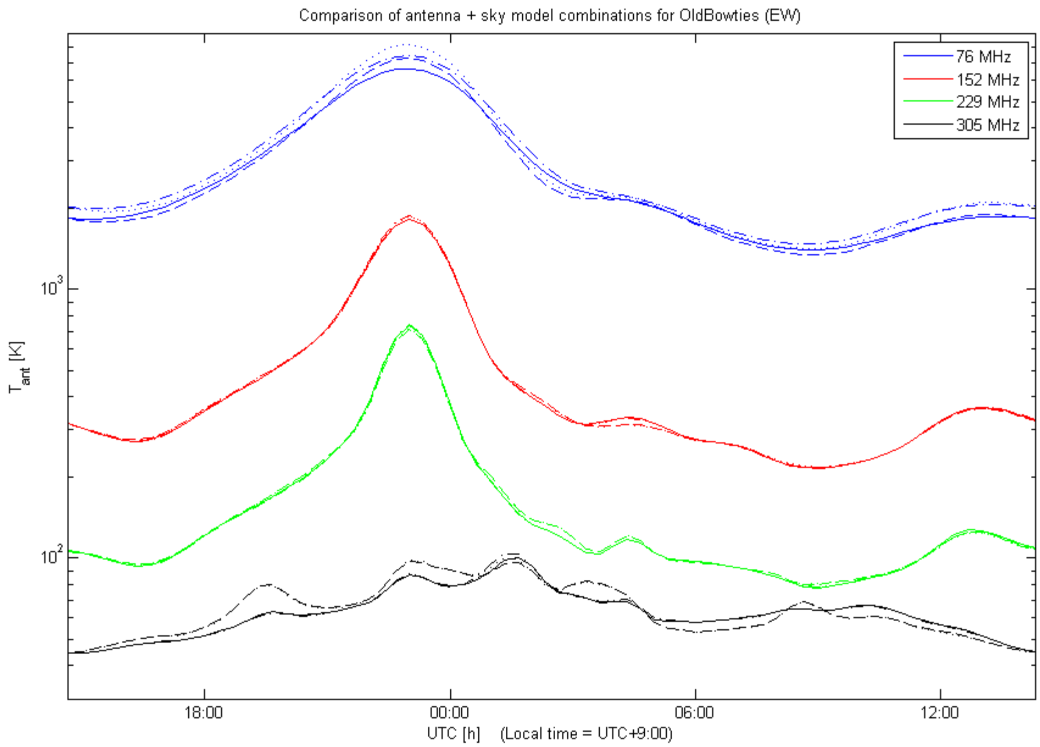

Figure 5. Same as Figure 3, but for the east-west polarization. In this case, the 305 MHz antenna patterns are dominated by north-south aligned sidelobes (as opposed to the east-west ones) and are less sensitive to the positions of the Galactic center and Sun.

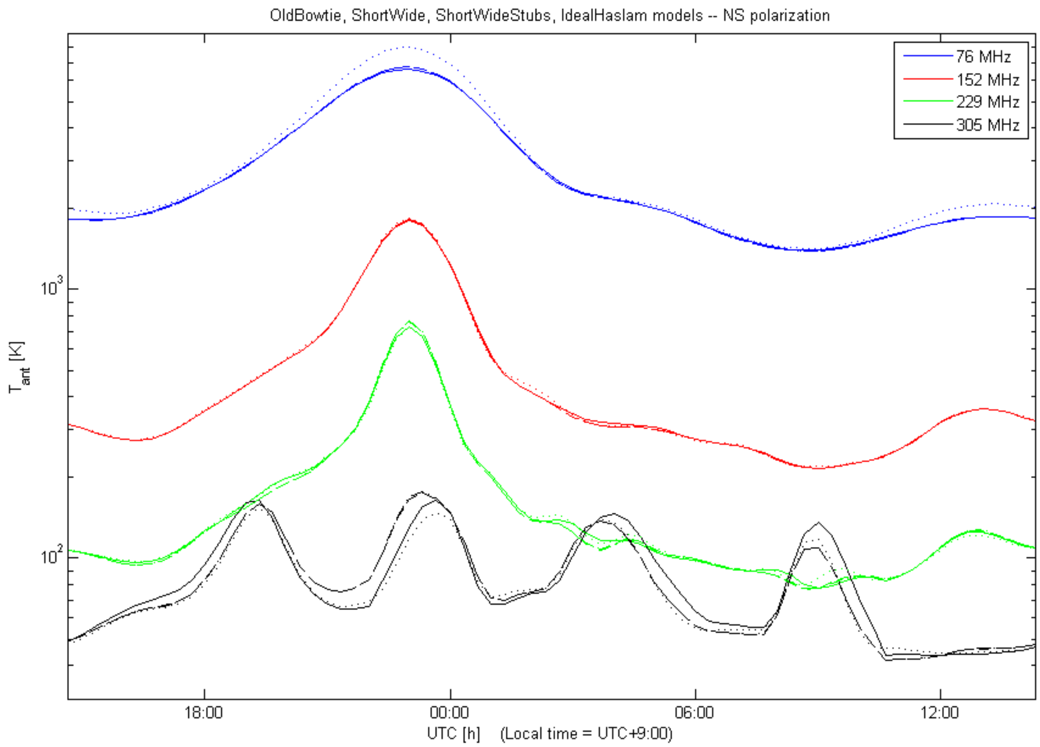

Figure 6. Comparison of the predicted drift scans for the north-south polarization of the four actual models used in the drift scan analysis. The solid lines are for the "OldBowtie" WIPL+GSM models. The dashed lines are for the "ShortWide" WIPL+GSM models. The dash-dot lines are for the "ShortWideStubs" WIPL+GSM models. And the dotted lines are for the ideal dipole + Haslam map models.

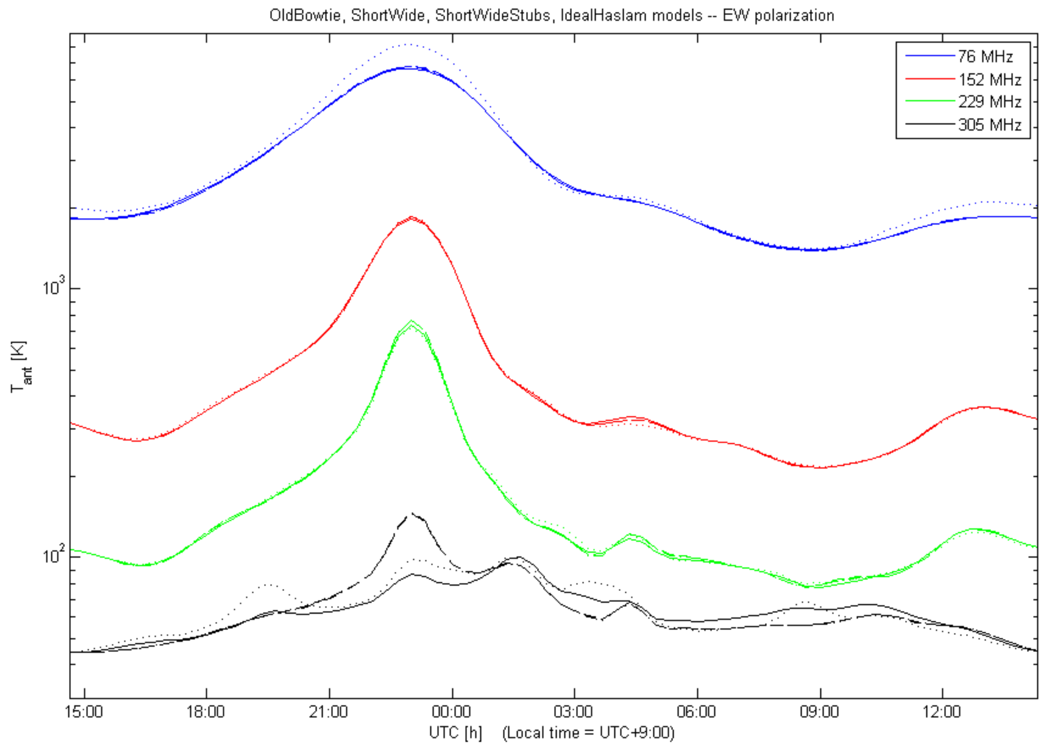

Figure 7. Same as Figure 6, but for the east-west polarization.

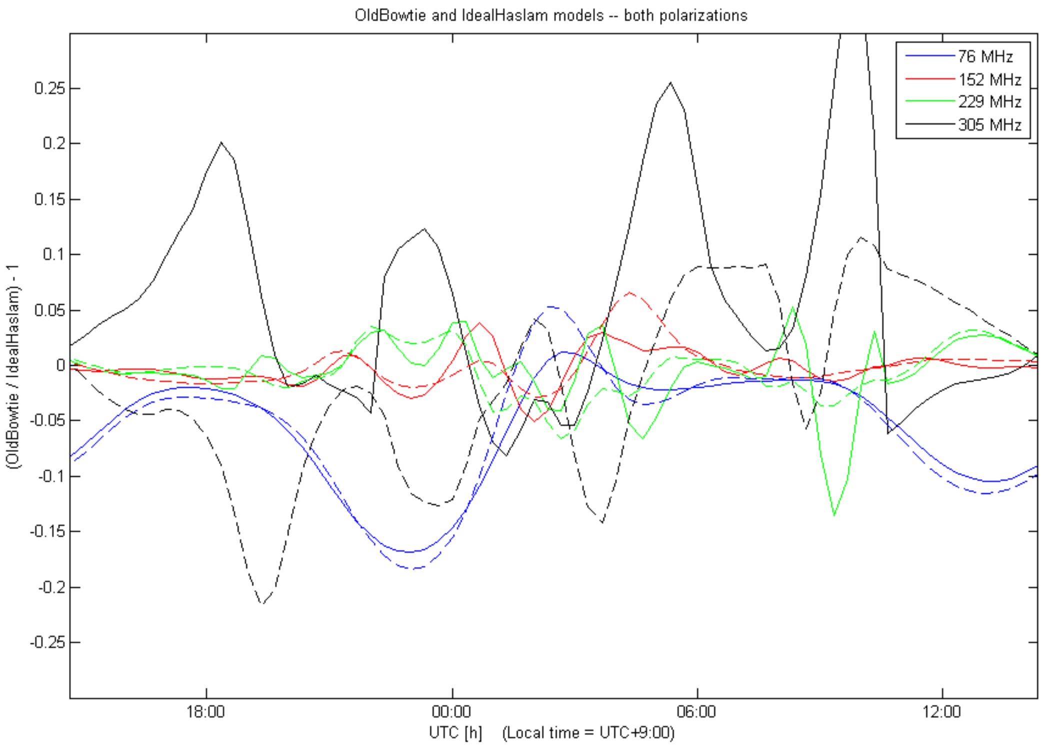

Figure 8. The fractional differences in the drift scans as a function of time between the "OldBowtie" WIPL+GSM models and the ideal dipole + Haslam map models for the four test frequencies. Solid lines are for the north-south polarization and dashed lines are for the east-west polarization.

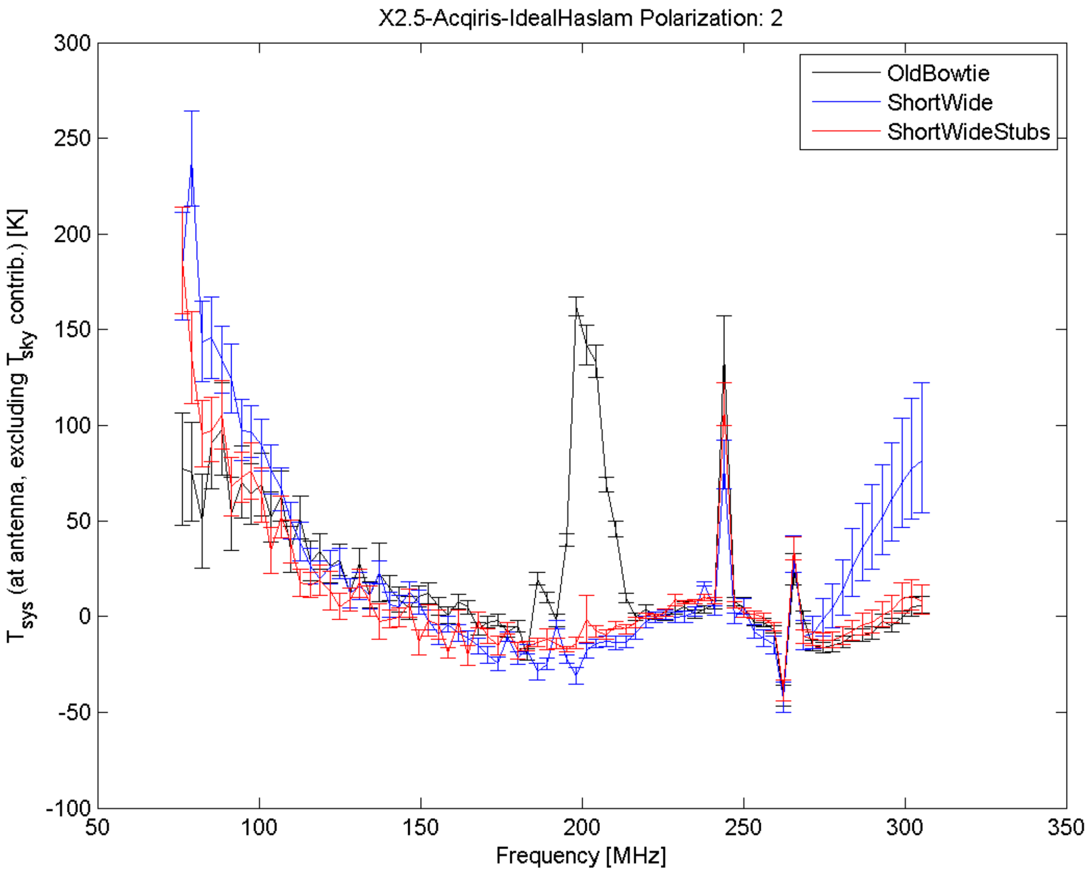

Figure 9. Derivation of the system temperature, Tsys, using the original ideal dipole + Haslam map models for each of the three dipole designs tested during X2.5. There are two discernable differences between the three dipole designs: 1) the large spike at 200 MHz is only present in the "OldBowtie" design, and 2) the "ShortWide" design seems to increase in Tsys more rapidly above 260 MHz than the other designs. Similarly, the "ShortWide" design does appear to have a slightly larger Tsys at low frequencies than the other designs (in particular, compared to the "ShortWideStubs" design which should have better impedance match at 100 MHz). The big glitches in all dipole designs at about 245 and 265 MHz are due to persistent RFI. It is also important to note the configuration of the final stage amplification after the beamformer and before the Acqiris spectrometer was not consistent between the drift scan measurements for the different dipole designs. According to Jamie Stevens, the number of amplifiers and attenuators was changed between drift scans until a reasonable signal-to-noise ratio was achieved. It is possible that some of the differences in this plot (and in Figures 10-12) could be due to changes in this configuration.

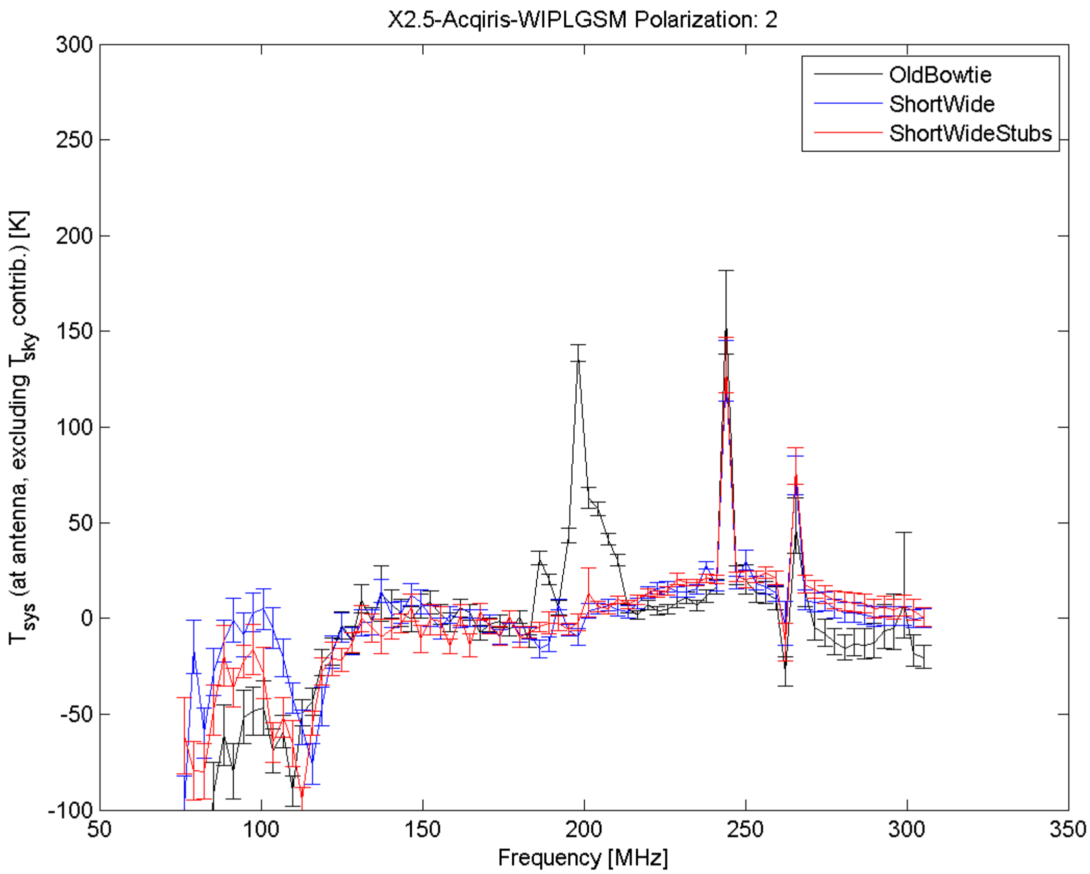

Figure 10. Same as Figure 9, but using the WIPL and GSM antenna and sky models in place of the original simple models. Again, we see that there is little distinguishable between the dipole designs except for the 200 MHz spike in the "OldBowtie" design. In this case, the "ShortWide" design does not seem to exhibit larger Tsys above 260 MHz than the other designs, but it does retain a slightly Tsys at low frequencies. Compared to Figure 9, the overall system temperature for all dipole designs in much lower for frequencies below 140 MHz using the new models than for the old models. In fact, it is unphysically low (below zero) over much of this range. Between 150 and 250 MHz, however, the two models (Figure 9 and Figure 10) seem to return fairly consistent results (but clearly not identical).

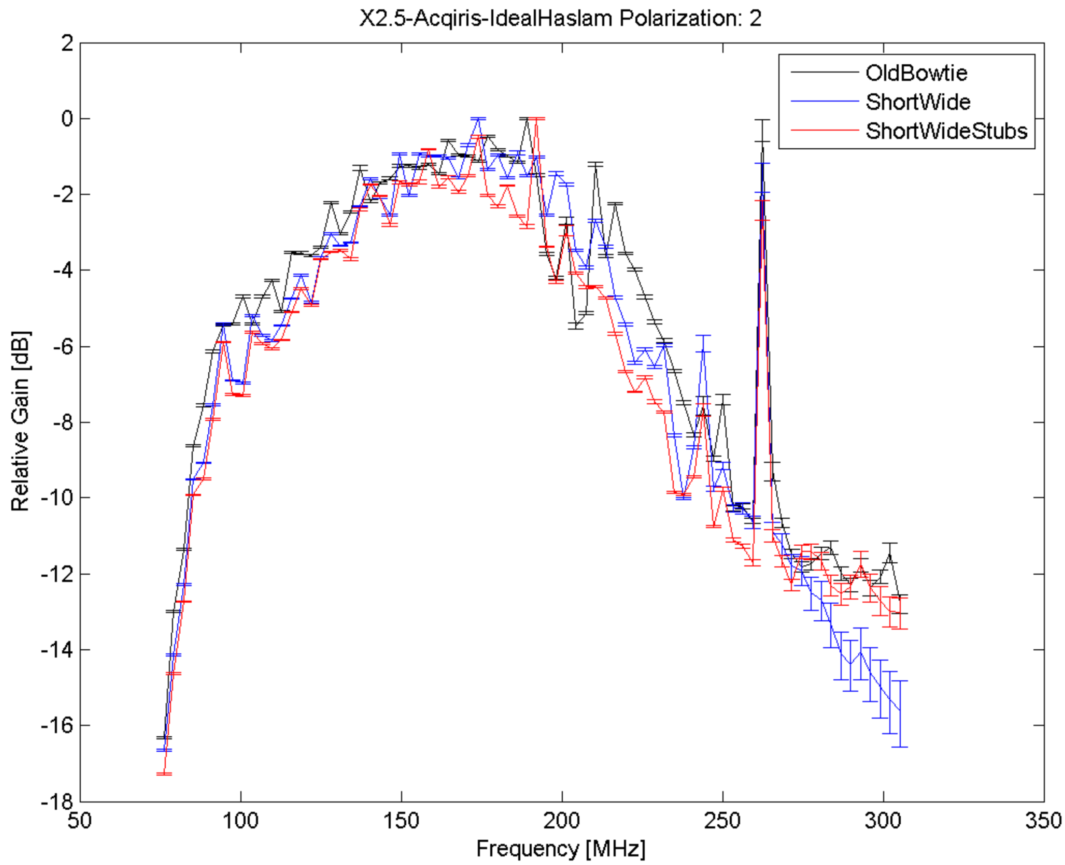

Figure 11. Comparison of the relative system gains for each of the dipole designs (colored lines) and both the old, simple antenna and sky models (top panel) and the new WIPL + GSM models (bottom panel). Each gain curve is normalized by dividing by its maximum gain value (which is typically around 150 MHz). Unfortunately, a direct comparison of absolute gains cannot be made since the final-stage amplifier configuration was modified between drift scans.

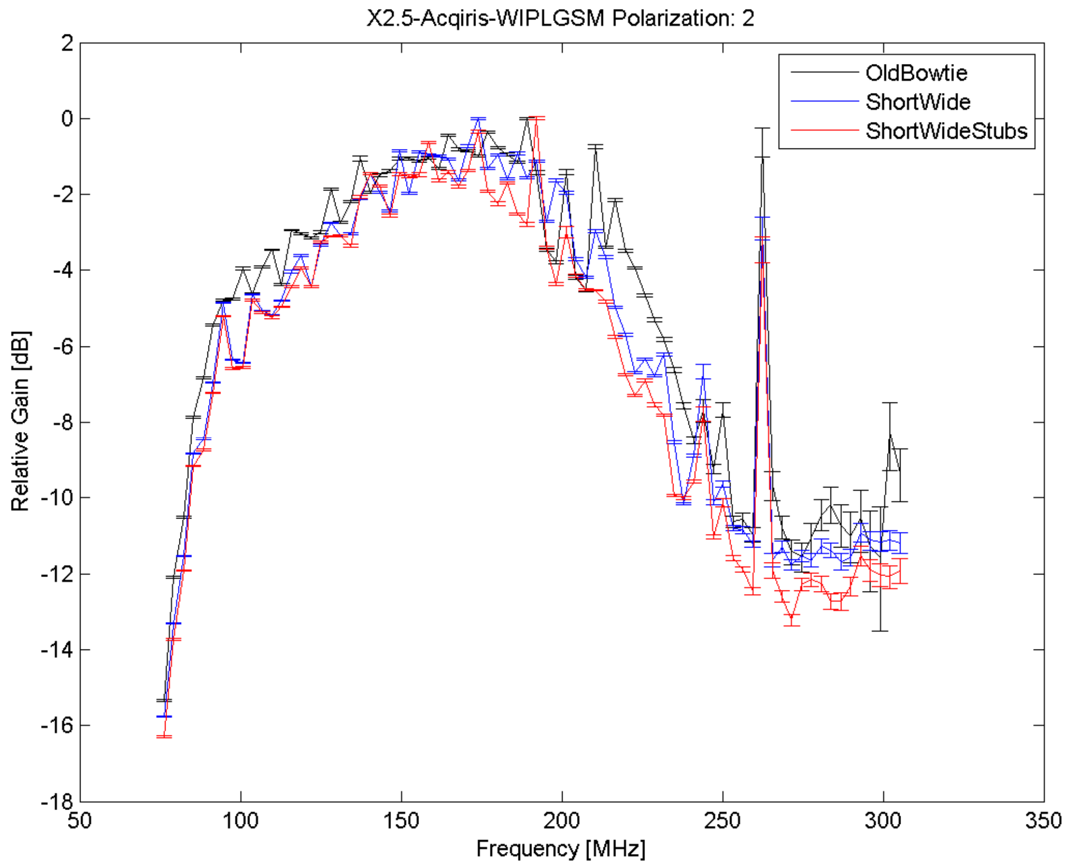

Figure 12. Same as Figure 11, but using the WIPL + GSM models.

Acknowledgements

This analysis was supported in many ways by the contributions of Jamie Stevens, David Herne, Merv Lynch, Chris Williams, Randall Wayth, Angelica de Oliveira-Costa, Frank Briggs, Brian Corey, Alan Rogers, and many others working on the MWA 32T system.

References

1. MWA-LFD Memo: Analysis of Drift Scans From 32T-X1 and Characterization of System Temperature
http://mwa-lfd.haystack.mit.edu/knowledgetree/view.php?fDocumentId=651

2. MWA-LFD Memo: Analysis of Drift Scans from 32T-X2
http://mwa-lfd.haystack.mit.edu/knowledgetree/view.php?fDocumentId=657

3. EDGES Memo #37/MWA-LFD Memo: Arrays with MWA and Modified MWA Antennas, Alan E. E. Rogers
http://www.haystack.mit.edu/ast/arrays/Edges/EDGES_memos/037.pdf

4. EDGES Memo #38/MWA-LFD Memo: Comparison of the MWA bowtie, shortwide and shortwide with stubs Antennas, Alan E. E. Rogers
http://www.haystack.mit.edu/ast/arrays/Edges/EDGES_memos/038.pdf

5. C. G. T. Haslam, H. Stoffel, C. J. Salter, and W. E. Wilson. A 408 MHz all-sky continuum survey. II - The atlas of contour maps. *A&AS*, 47:1 — +, January 1982

6. A. de Oliveira-Costa, M. Tegmark, B. M. Gaensler, J. Jonas, T. L. Landecker, P. Reich. A Model of Diffuse Galactic Radio Emission from 10 MHz to 100 GHz, 2008 (arXiv:0802.1525)

Apendix A: “OldBowtie” Results (WIPL + GSM)

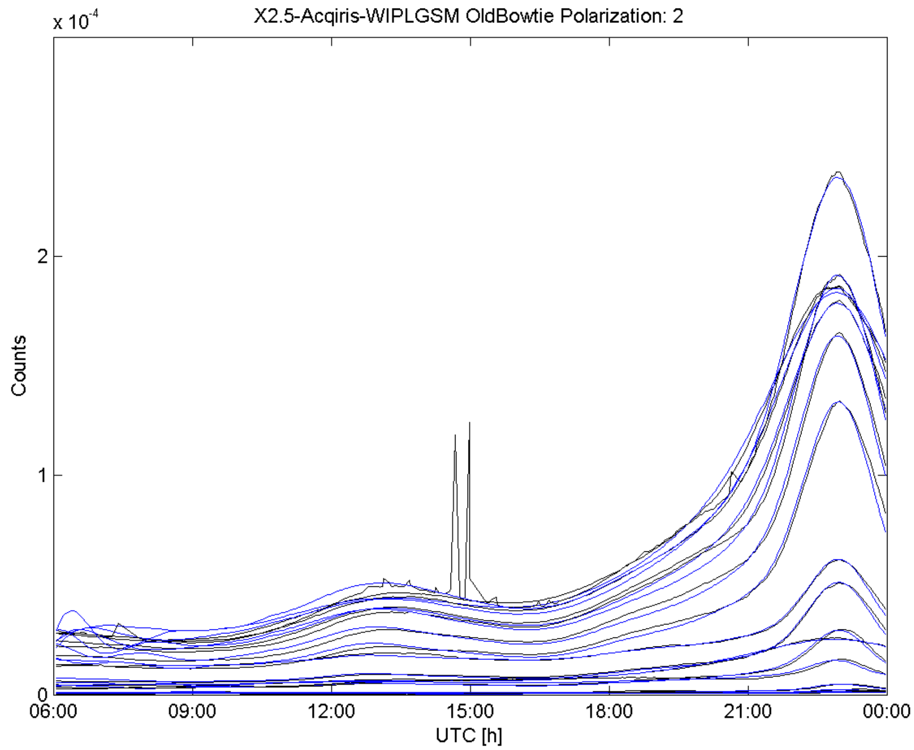
X2.5-Acqiris-WIPLGSM OldBowtie Polarization: 2
x 10^-4
Counts
UTC [h]
0
1
2
06:00
09:00
12:00
15:00
18:00
21:00
00:00

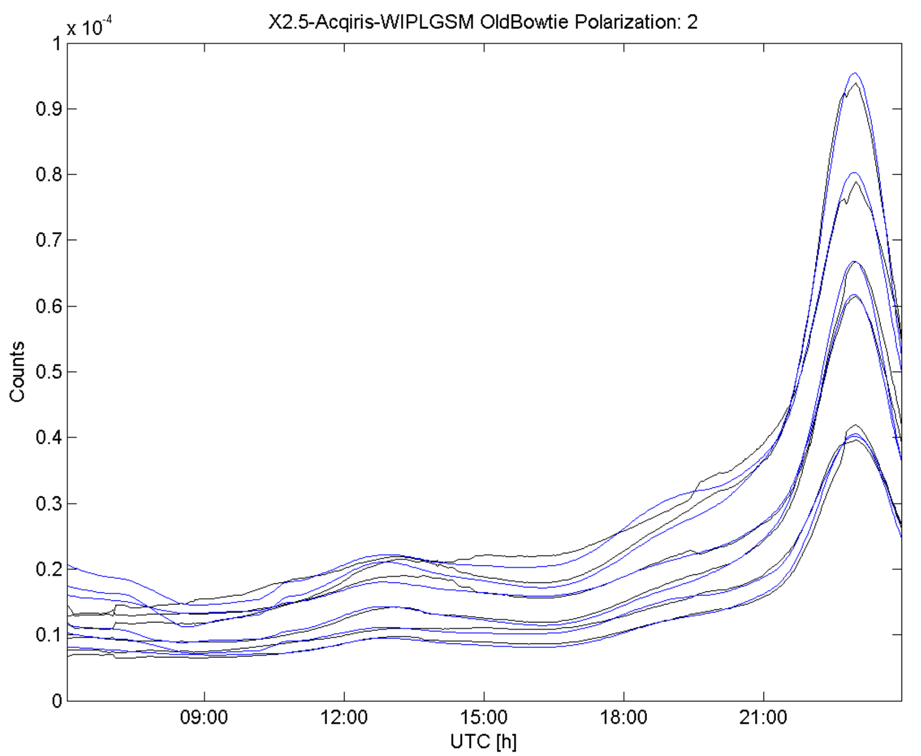
X2.5-Acqiris-WIPLGSM OldBowtie Polarization: 2
x 10^-4
Counts
UTC [h]
0
0.1
0.2
0.3
0.4
0.5
0.6
0.7
0.8
0.9
1
09:00
12:00
15:00
18:00
21:00

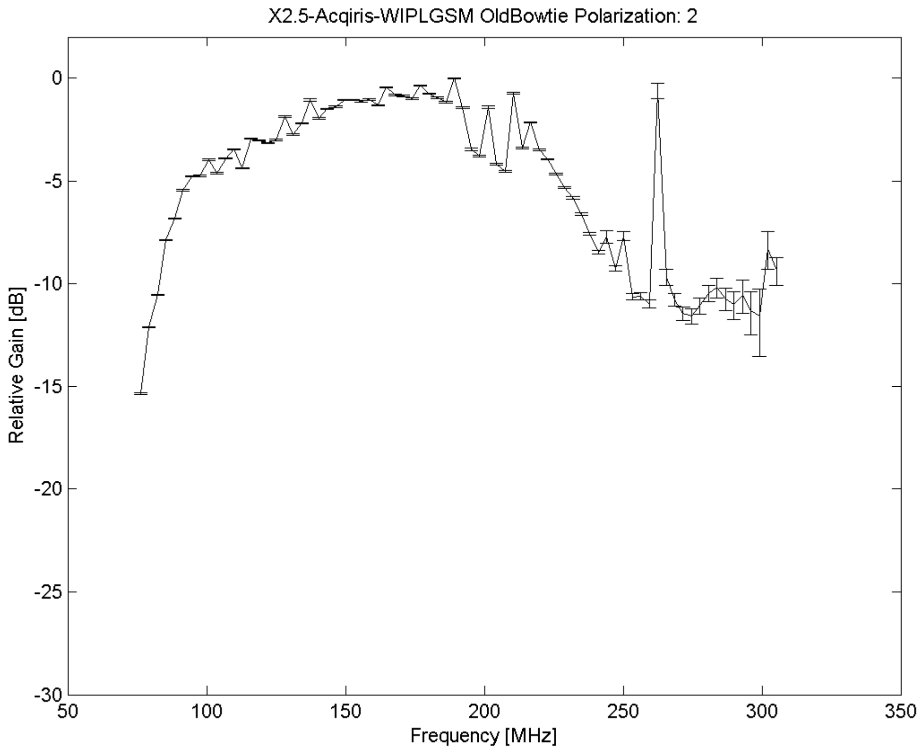
X2.5-Acqiris-WIPLGSM OldBowtie Polarization: 2
Relative Gain [dB]
Frequency [MHz]
0
-5
-10
-15
-20
-25
-30
50
100
150
200
250
300
350

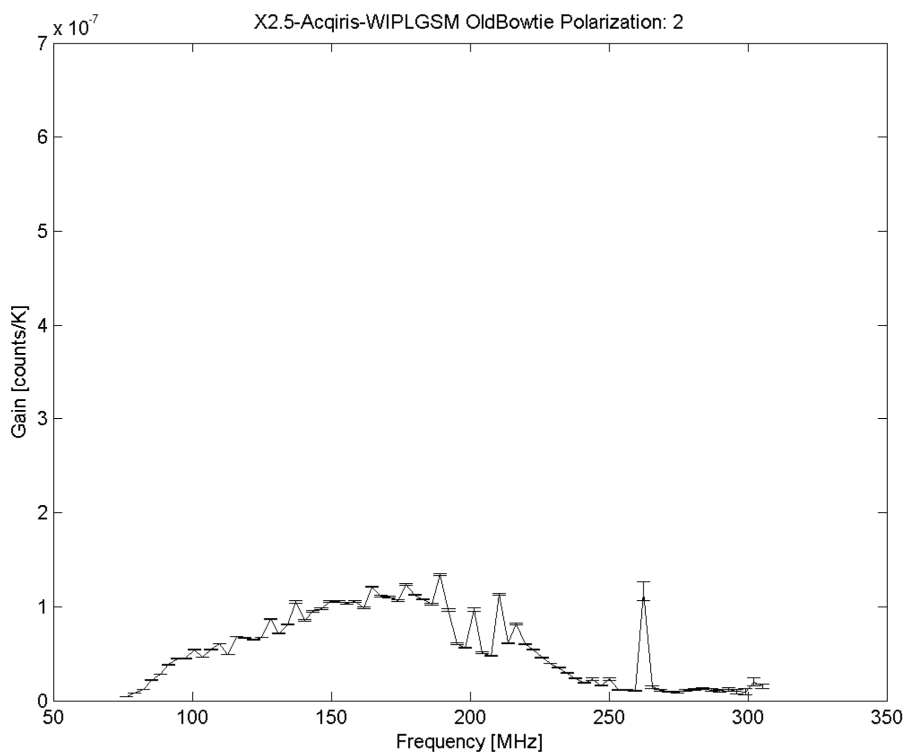
X2.5-Acqiris-WIPLGSM OldBowtie Polarization: 2
x 10^-7
Gain [counts/K]
Frequency [MHz]
0
1
2
3
4
5
6
7
50
100
150
200
250
300
350

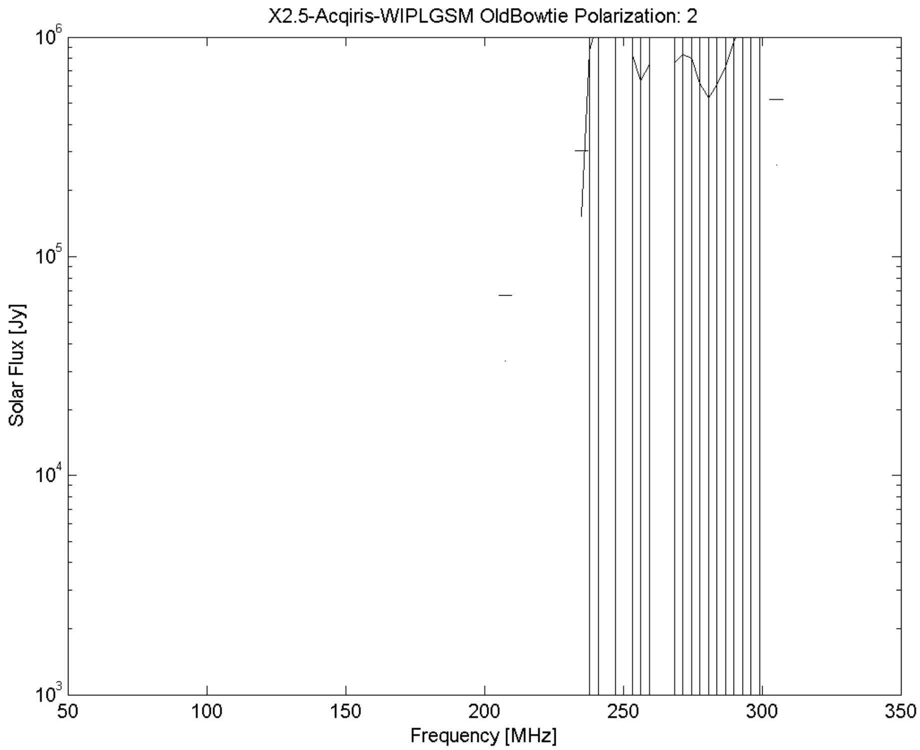
X2.5-Acqiris-WIPLGSM OldBowtie Polarization: 2
Solar Flux [Jy]
Frequency [MHz]

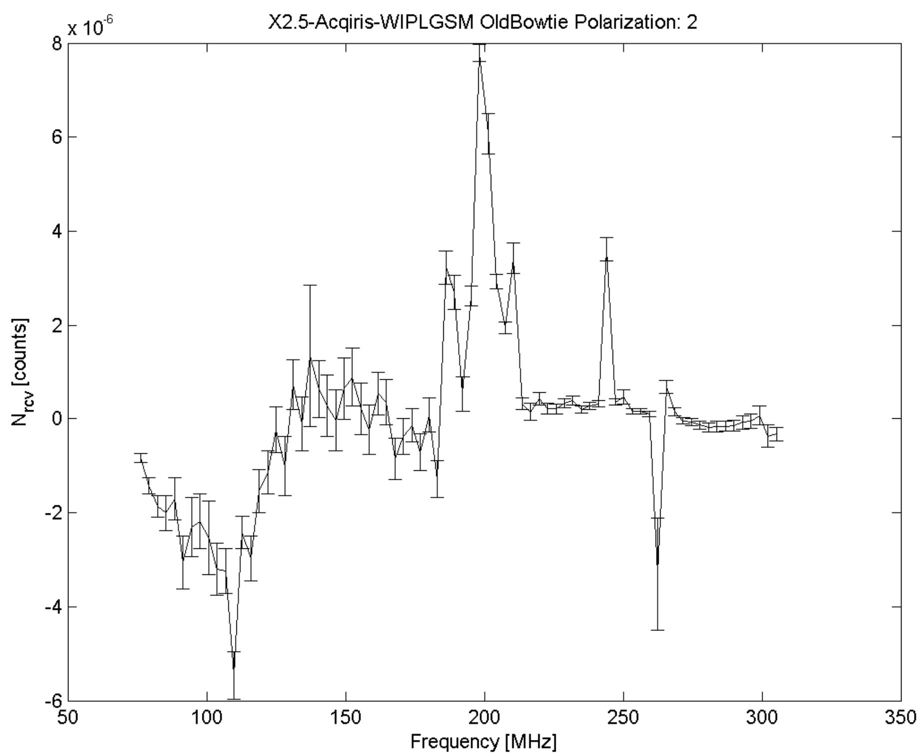
X2.5-Acqiris-WIPLGSM OldBowtie Polarization: 2
x 10^-6
N_rcv [counts]
Frequency [MHz]

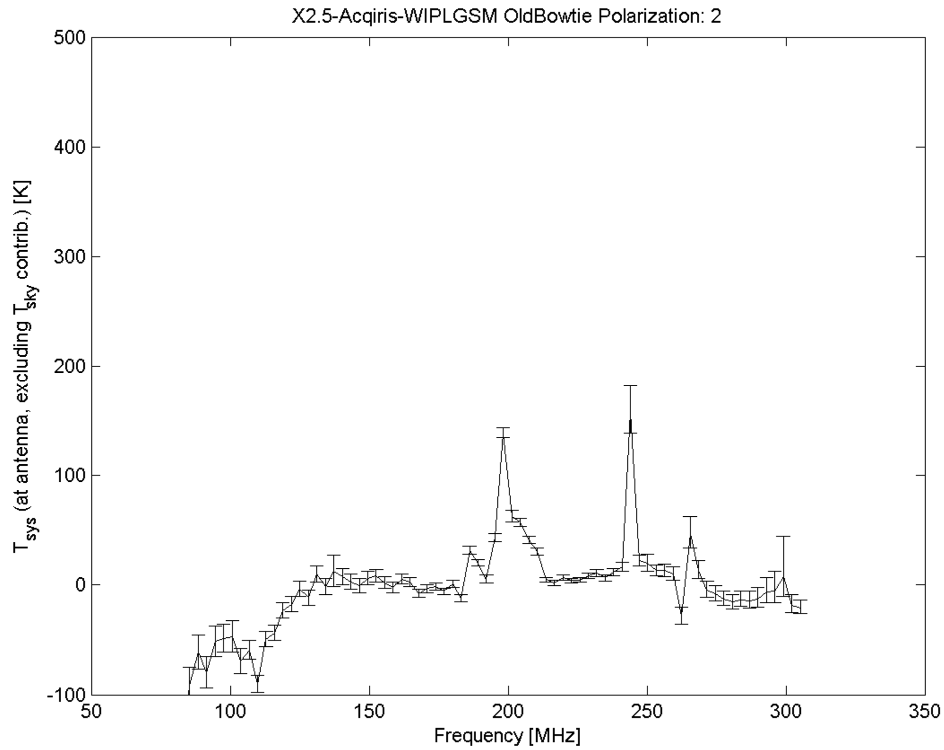
X2.5-Acqiris-WIPLGSM OldBowtie Polarization: 2
T_{sys} (at antenna, excluding T_{sky} contrib.) [K]
Frequency [MHz]
500
400
300
200
100
0
-100
50
100
150
200
250
300
350

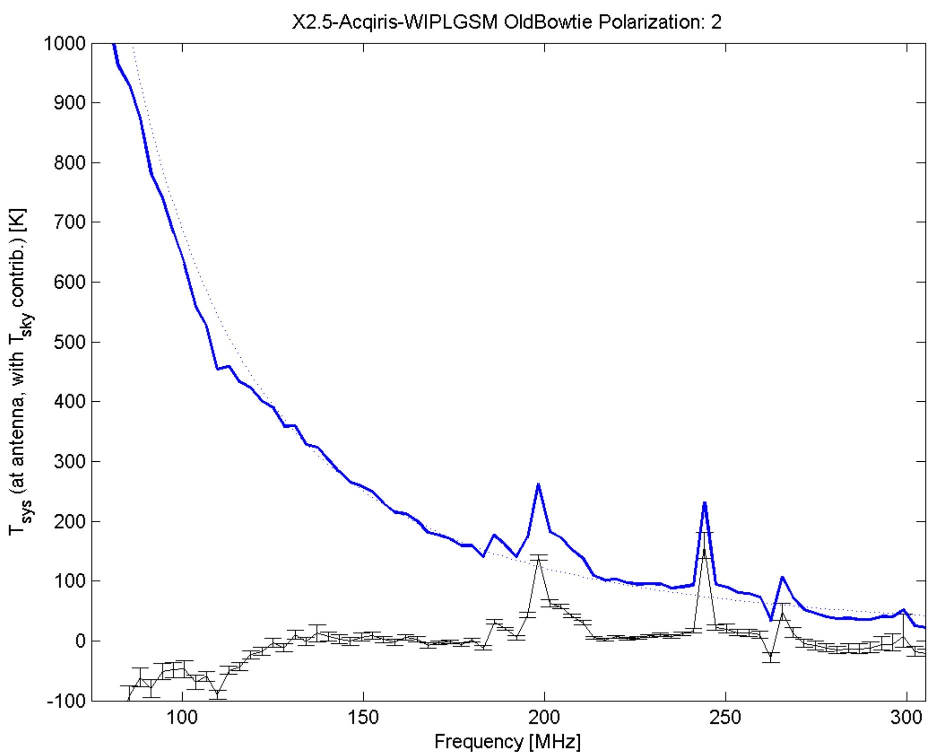
X2.5-Acqiris-WIPLGSM OldBowtie Polarization: 2
T_{sys} (at antenna, with T_{sky} contrib.) [K]
Frequency [MHz]
1000
900
800
700
600
500
400
300
200
100
0
-100
100
150
200
250
300

Apendix B: “ShortWide” Results (WIPL + GSM)

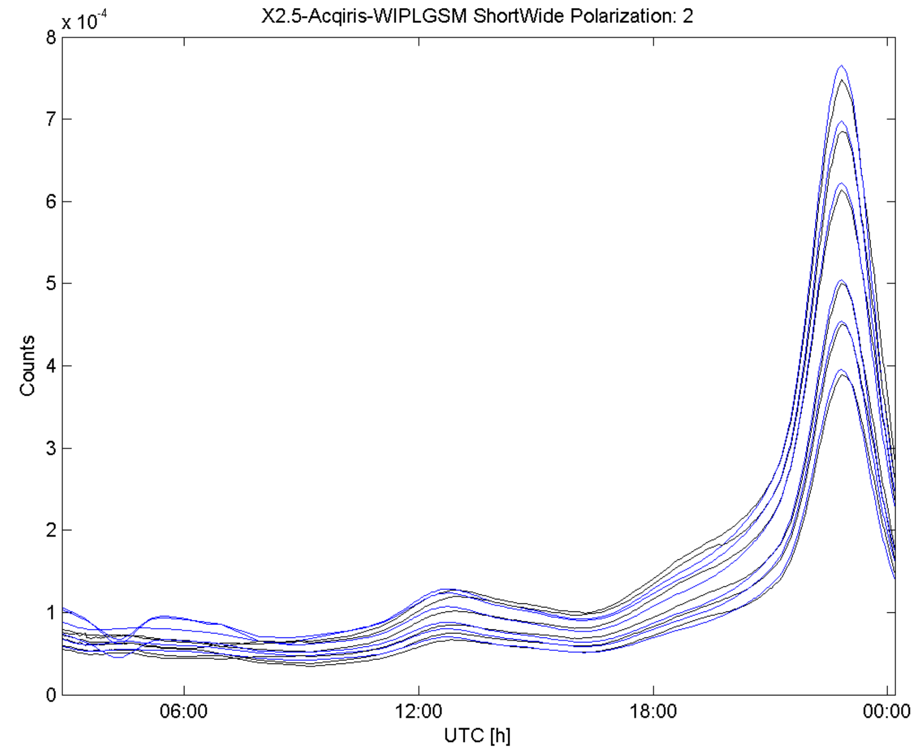

X2.5-Acqiris-WIPLGSM ShortWide Polarization: 2
x 10^-4
0
1
2
3
4
5
6
7
8
Counts
06:00
12:00
18:00
00:00
UTC [h]

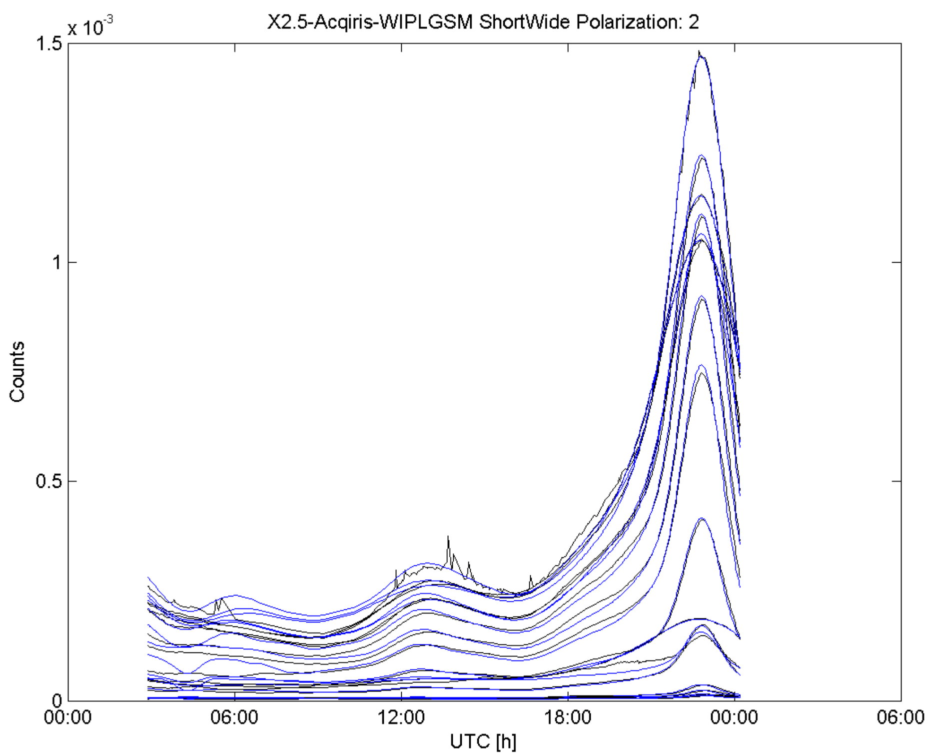

X2.5-Acqiris-WIPLGSM ShortWide Polarization: 2
x 10^-3
0
0.5
1
1.5
Counts
00:00
06:00
12:00
18:00
00:00
06:00
UTC [h]

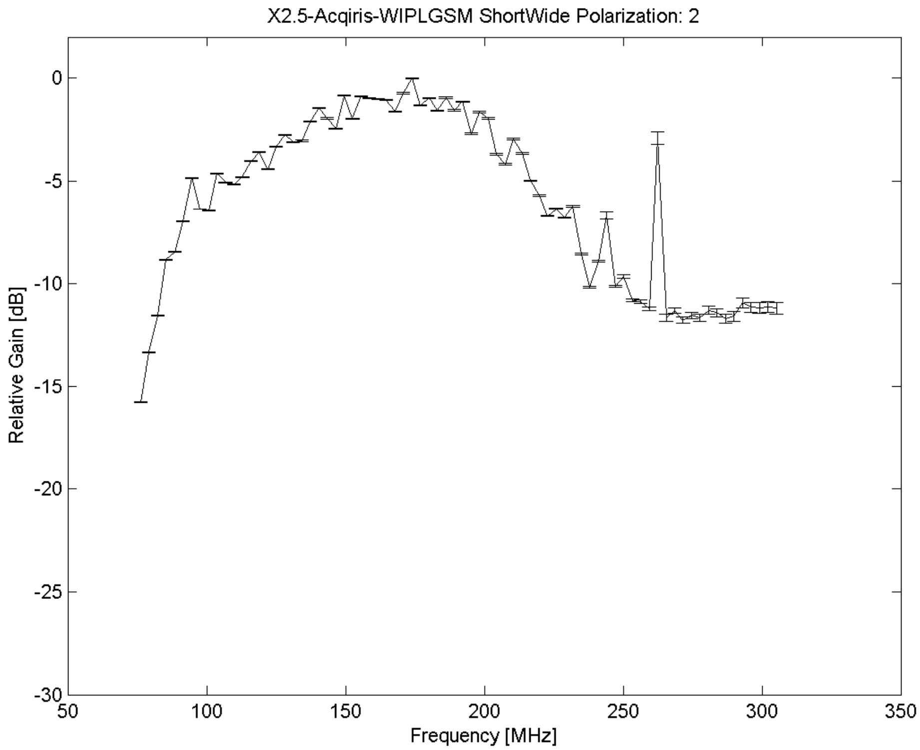

X2.5-Acqiris-WIPLGSM ShortWide Polarization: 2
Relative Gain [dB]
Frequency [MHz]
0
-5
-10
-15
-20
-25
-30
50
100
150
200
250
300
350

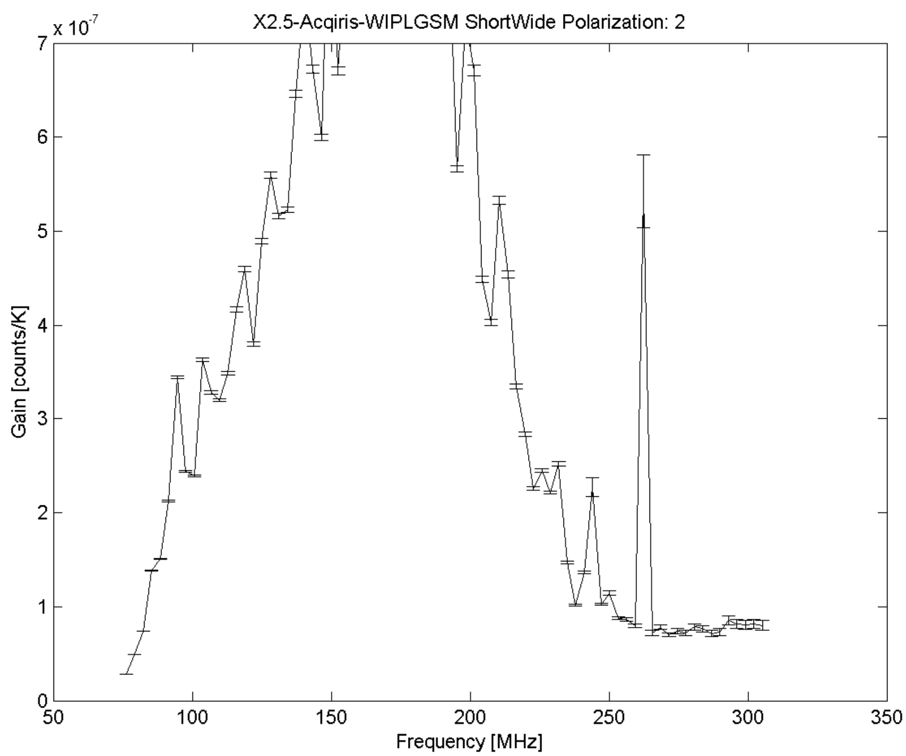

X2.5-Acqiris-WIPLGSM ShortWide Polarization: 2
x 10^-7
Gain [counts/K]
Frequency [MHz]
0
1
2
3
4
5
6
7
50
100
150
200
250
300
350

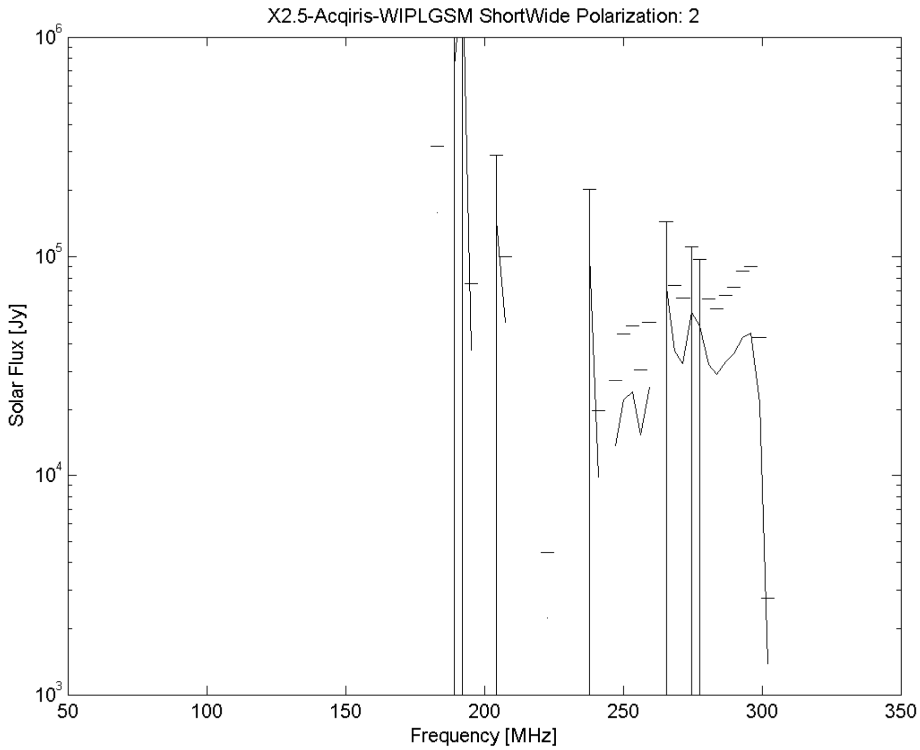
X2.5-Acqiris-WIPLGSM ShortWide Polarization: 2
Solar Flux [Jy]
Frequency [MHz]
50
100
150
200
250
300
350

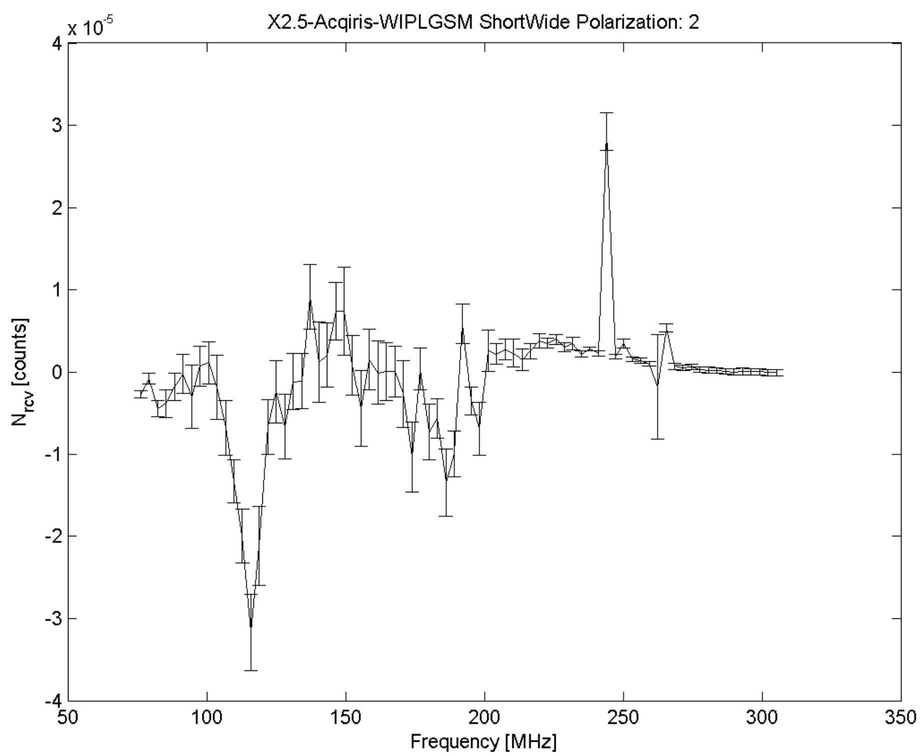
X2.5-Acqiris-WIPLGSM ShortWide Polarization: 2
x 10-5
N rcv [counts]
Frequency [MHz]
4
3
2
1
0
-1
-2
-3
-4
50
100
150
200
250
300
350

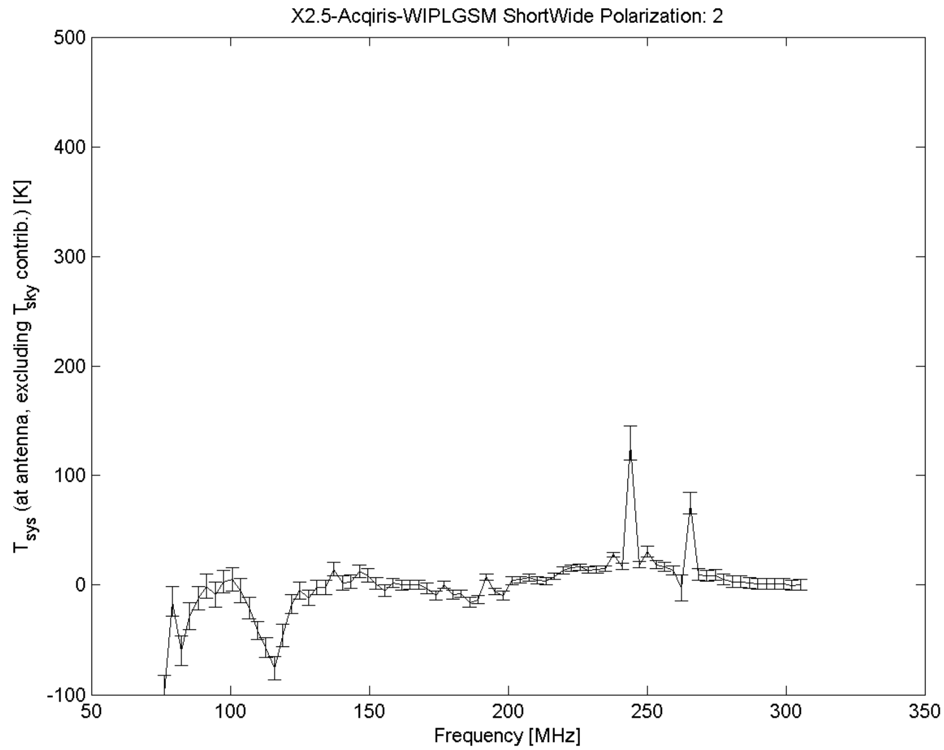

X2.5-Acqiris-WIPLGSM ShortWide Polarization: 2
T_sys (at antenna, excluding T_sky contrib.) [K]
Frequency [MHz]
500
400
300
200
100
0
-100
50
100
150
200
250
300
350

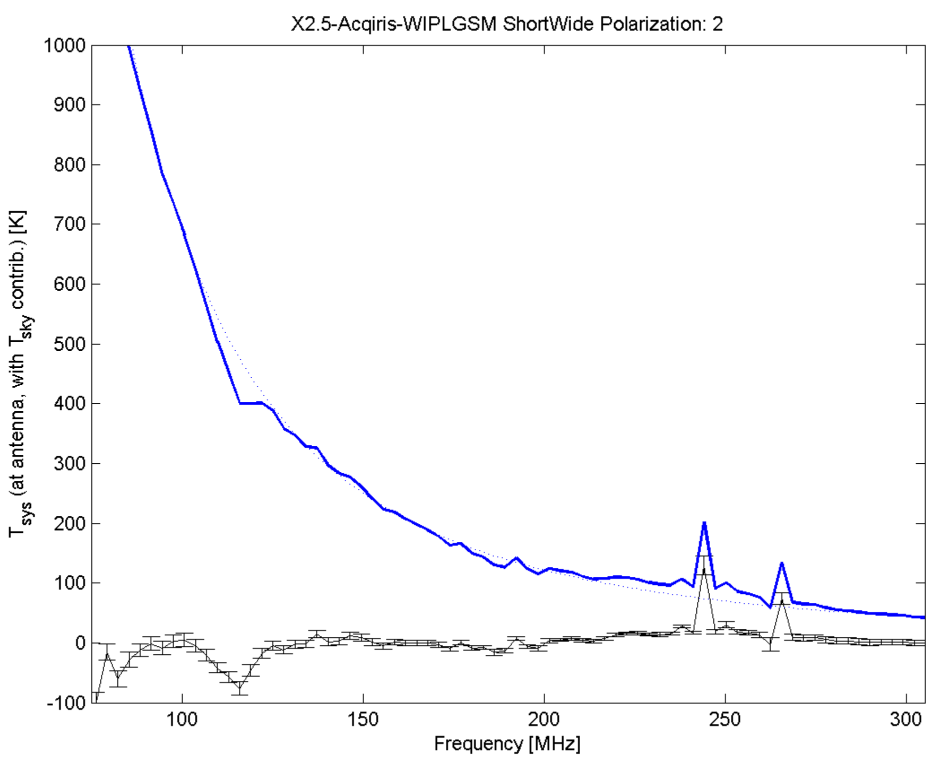

X2.5-Acqiris-WIPLGSM ShortWide Polarization: 2
T_sys (at antenna, with T_sky contrib.) [K]
Frequency [MHz]
1000
900
800
700
600
500
400
300
200
100
0
-100
100
150
200
250
300

Apendix C: “ShortWideStubs” Results (WIPL + GSM)

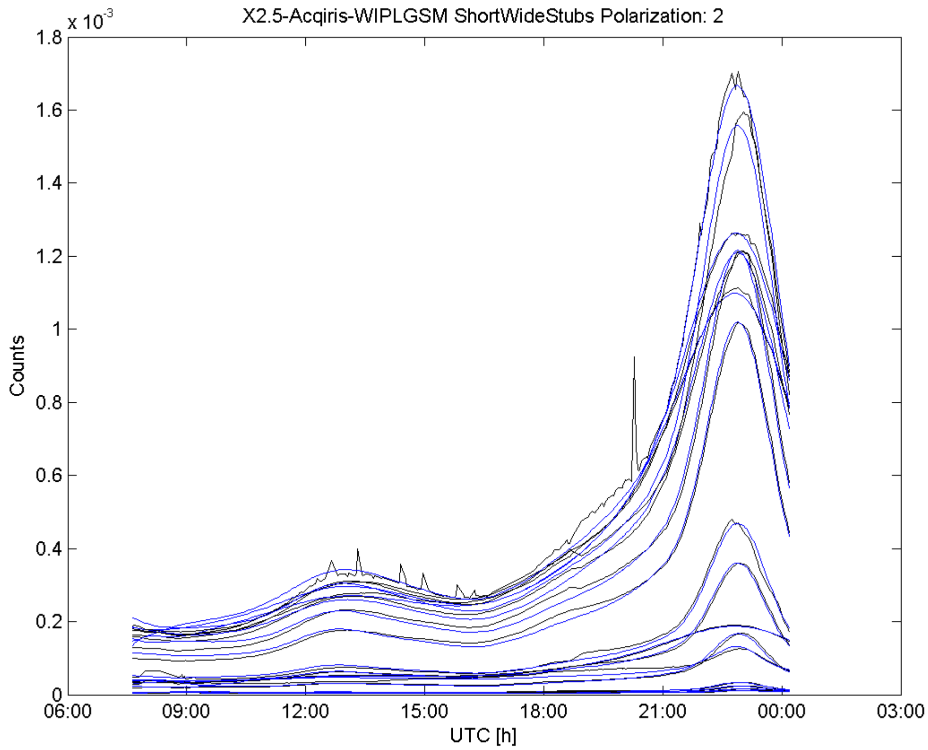
X2.5-Acqiris-WIPLGSM ShortWideStubs Polarization: 2
x 10^-3
1.8
1.6
1.4
1.2
1
0.8
0.6
0.4
0.2
0
Counts
06:00
09:00
12:00
15:00
18:00
21:00
00:00
03:00
UTC [h]

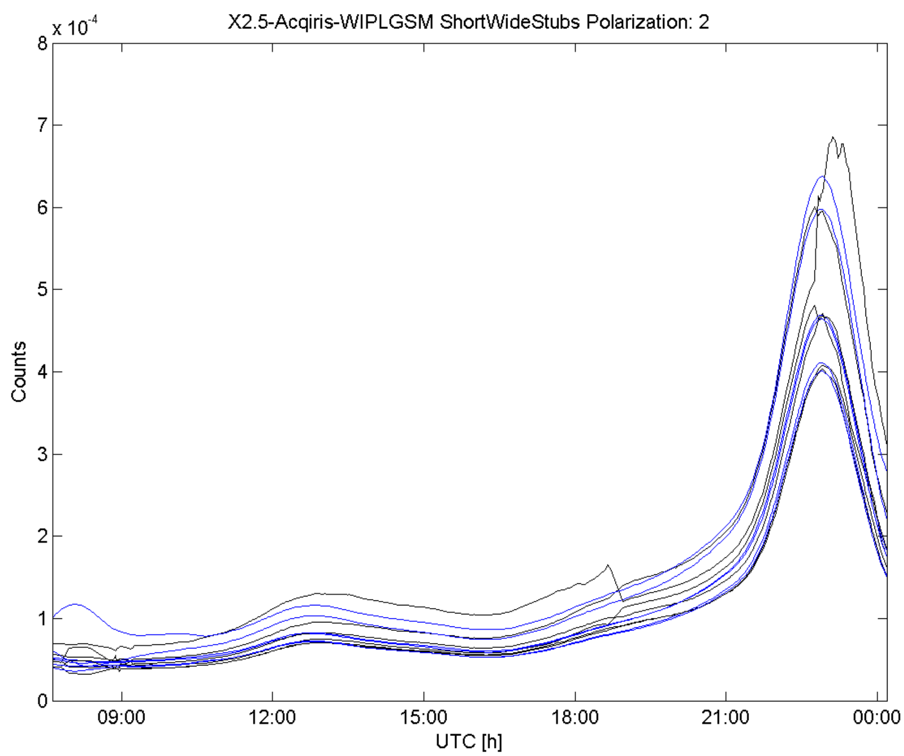
X2.5-Acqiris-WIPLGSM ShortWideStubs Polarization: 2
x 10^-4
8
7
6
5
4
3
2
1
0
Counts
09:00
12:00
15:00
18:00
21:00
00:00
UTC [h]

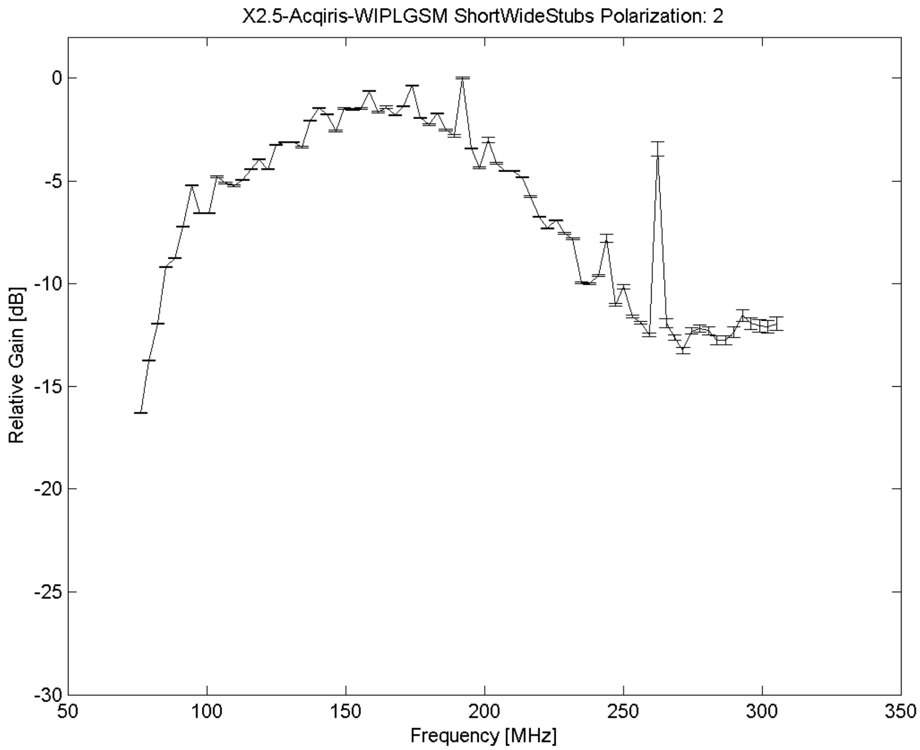
X2.5-Acqiris-WIPLGSM ShortWideStubs Polarization: 2
Relative Gain [dB]
Frequency [MHz]
0
-5
-10
-15
-20
-25
-30
50
100
150
200
250
300
350

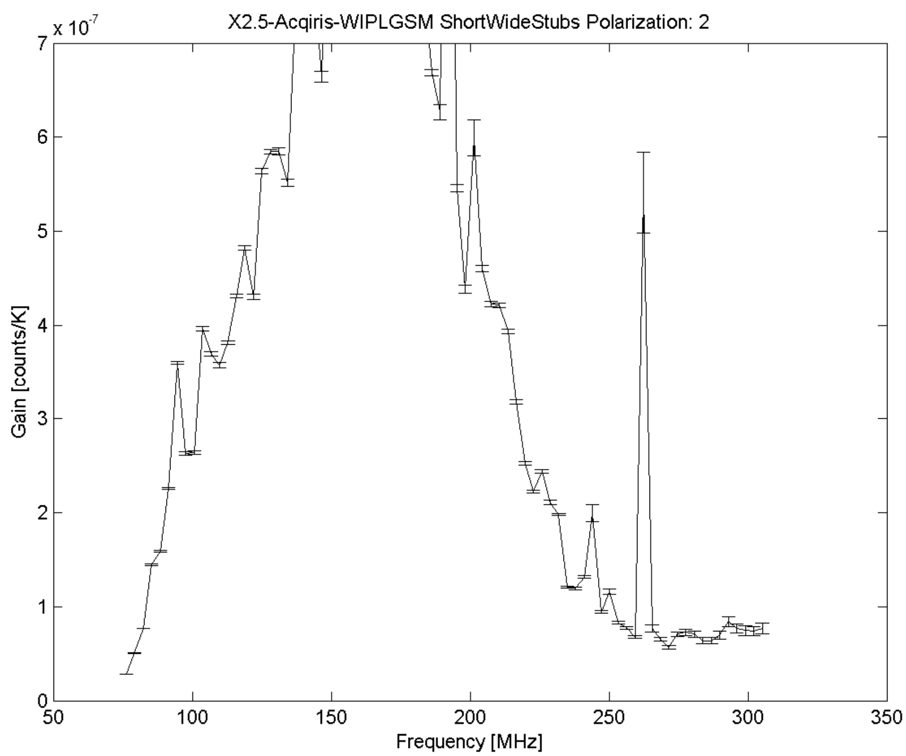
X2.5-Acqiris-WIPLGSM ShortWideStubs Polarization: 2
x 10^-7
Gain [counts/K]
Frequency [MHz]
7
6
5
4
3
2
1
0
50
100
150
200
250
300
350

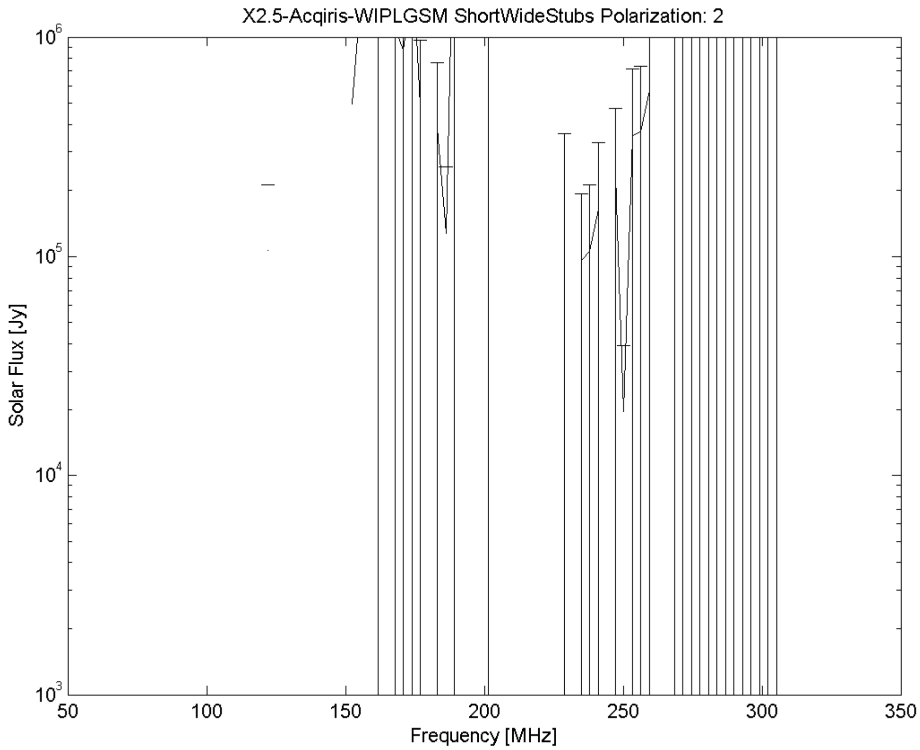

X2.5-Acqiris-WIPLGSM ShortWideStubs Polarization: 2
Solar Flux [Jy]
Frequency [MHz]

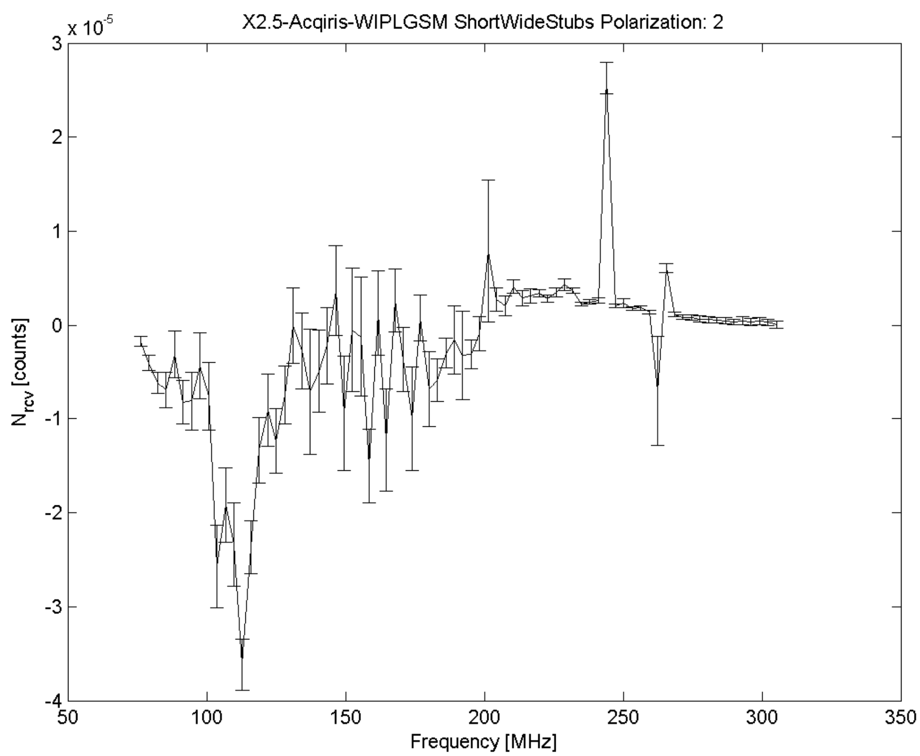

X2.5-Acqiris-WIPLGSM ShortWideStubs Polarization: 2
x 10^-5
N_rcv [counts]
Frequency [MHz]

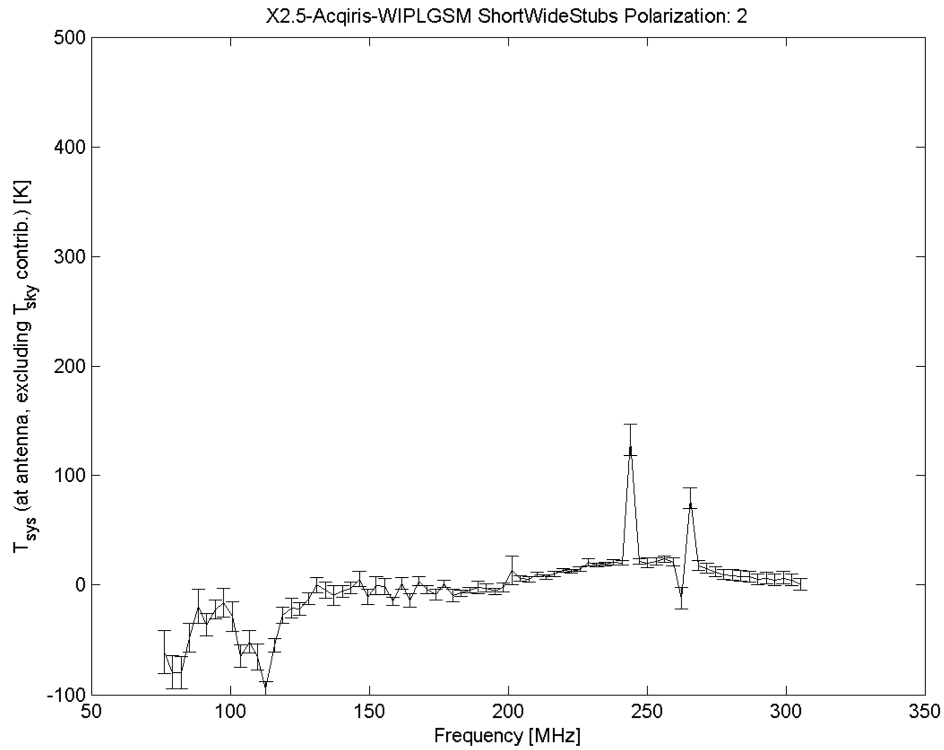
X2.5-Acqiris-WIPLGSM ShortWideStubs Polarization: 2
T_{sys} (at antenna, excluding T_{sky} contrib.) [K]
Frequency [MHz]

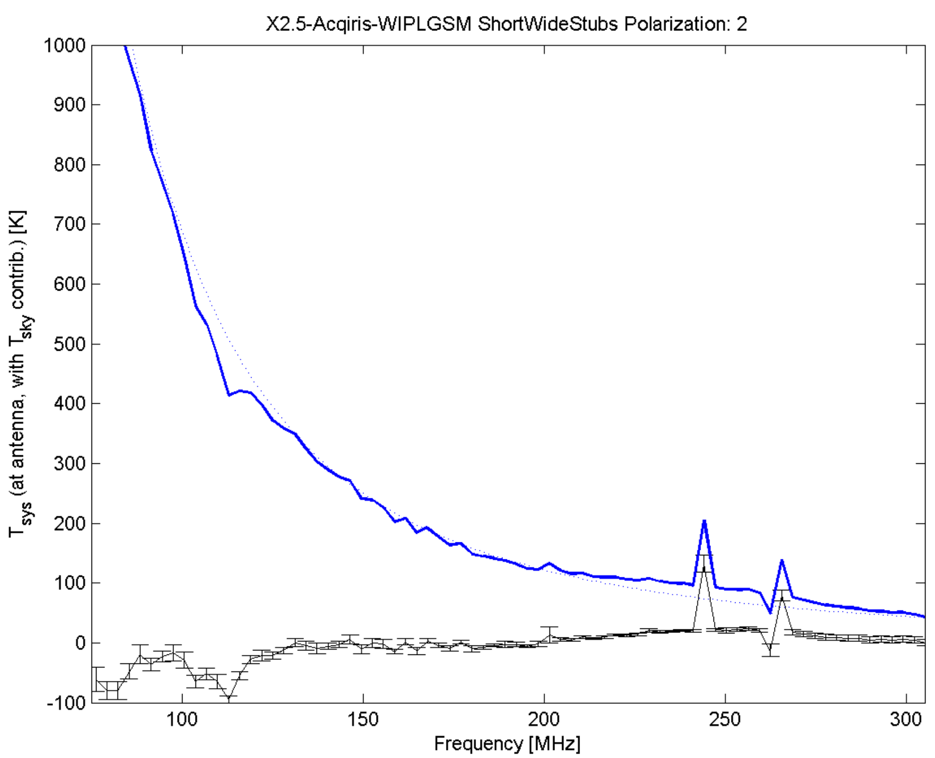
X2.5-Acqiris-WIPLGSM ShortWideStubs Polarization: 2
T_{sys} (at antenna, with T_{sky} contrib.) [K]
Frequency [MHz]